Increased Land Subsidence and Sea-Level Rise are Submerging Egypt's Nile Delta Coastal Margin

Jean-Daniel Stanley, *Mediterranean Basin (MEDIBA) Program, 6814 Shenandoah Court, Adamstown, Maryland 21710, USA, stanleyd1@outlook.com; and* ***Pablo L. Clemente,*** *Dept. of Geographic and Environmental Systems, University of Maryland, Baltimore County, 1000 Hilltop Circle, Baltimore, Maryland 21250, USA, clempa1@umbc.edu*

ABSTRACT

Egypt's Nile delta, only ~1 m above mean sea level at the Mediterranean coast, is subject to uneven rates of submergence. This is a response to several factors leading to increasing land lowering (subsidence) of the northern delta and adjacent seafloor, plus an accelerating rise in eustatic (world) sea level in the Mediterranean. An average eustatic sea-level rise of ~3 mm/yr represents only ~26% to 45% of total *relative sea-level rise* measured along this margin. Three factors leading to subsidence are neotectonic lowering, compaction of Holocene sequences, and diminished sediment replenishment by much reduced Nile flow to Egypt's coast. Subsidence accounts for variable average land lowering of ~3.7 mm/yr of section in the NW delta, ~7.7 mm/yr in the N delta, and ~8.4 mm/yr in the NE delta, based on compaction rates of strata thicknesses that decrease down-core between top and base of Holocene sections in 85 drill cores distributed along the delta margin. Among present critical challenges are marked reduction of Nile water and sediment below the High Aswan Dam that can now reach the delta coast. It is expected that problems of fresh water and energy poverty in the lower Nile Basin are likely to be seriously exacerbated in years ahead by construction of Ethiopia's Grand Renaissance Dam (GERD). Completion of this, the biggest hydroelectric structure in Africa, is this year. Egypt, the Sudan, and Ethiopia must resolve the looming crisis of diminished Blue Nile water and sediment distribution to the lower Nile Basin and Egypt's delta margin.

INTRODUCTION

Recent submergence of many world fluvial-marine deltaic margins is generally attributed to increased eustatic (world) sea-level rise responding largely to increased polar glacial ice melt and thermal expansion of seawater associated with global warming (Hansen et al., 2016). Less attention has been paid to other mechanisms that could presently play a substantial, or even greater, role in a delta's coastal submergence. The Nile delta's margin in northern Egypt is examined here with regard to its ongoing submergence by rising sea level (Shaltout et al., 2015), combined with the effects of land subsidence near its Mediterranean coastline and seafloor offshore (Fig. 1). The latter include (1) effects of recent neotectonic lowering of the delta surface associated with substrate displacement; (2) ongoing compaction of the Holocene sedimentary sequence; and (3) diminished sediment replenishment by the Nile River at the delta coast and adjacent shelf. We propose that these three phenomena have triggered a greater amount of subsidence of the low-elevation delta margin (~1 m above mean sea level [msl]) and consequent landward coastline retreat during the past few thousand years than could have been produced during this time span by the increased rate of eustatic sea-level rise alone. Factors triggering land subsidence, interacting with increased rise in eustatic sea level, account for what is generally termed *relative sea-level rise*.

This survey highlights increased anthropogenic pressures that augment the impact of these factors and have negative consequences for populations in the northern delta. Of major concern is the ongoing reduction of useable land and fresh water needed for agricultural production in this small but vital breadbasket, one that has previously accounted for 60% of the country's food production. This continued coastal margin submergence occurs at a time when Egypt, facing increased economic stress and diminished internal political stability (La Guardia, 2016), must already import much of its food to feed its growing population concentrated in the Nile delta and valley.

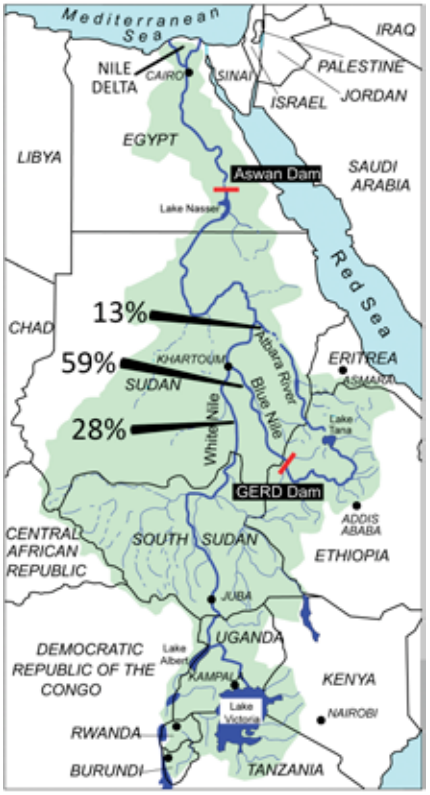

Figure 1. Map of the Nile Basin indicating relative percentages of fresh-water flow contributed by the Blue Nile, Atbara River, and the White Nile to the Main Nile in the Sudan and Egypt. GERD—Grand Ethiopian Renaissance Dam.

BACKGROUND

The Nile Basin covers 3,250,000 km^2 and extends northward across 36° of latitude. The delta forms at the mouth of the Nile, the world's longest river (~6700 km), whose water in Egypt is derived from two north-flowing branches, the Blue and White Niles, that merge as the Main Nile in the northern Sudan (Fig. 1). Interpretations regarding Holocene depositional

sequences at the delta's coastal margin (Fig. 2A) are based on stratigraphic, sedimentological, petrologic, biogenic, and geochemical analyses of >3000 samples selected from 85 radiocarbon-dated drill cores (dots in Fig. 2B). These cores and supplemental study materials were examined during the past 30 years by the Smithsonian Institution's Mediterranean Basin (MEDIBA) Program (Stanley et al., 1996; Stanley and Warne, 1998). Total core lengths range from 20 m to >50 m from the delta surface downward, with many sections radiocarbon dated to provide a chrono-stratigraphic framework. The upper part of the Late Pleistocene's largely sandy sections (Mit Ghamer Fm.) is generally recovered at most core bases; these older sections, in turn, are covered by Holocene nutrient-rich silty mud and fine sand sequences (Bilquas Fm.) that thicken northward and eastward along the coast (Fig. 2B). Core sites are distributed from east to west in a curvilinear, coast-parallel area of ~7000 km^2 that forms the northern third of the delta; most sites are positioned <30 km from the present arcuate shoreline at elevations to ~1 m or lower above msl.

Additional data are derived from other sources: cores obtained by others in the delta (Attia, 1954; Marriner et al., 2012); sediment grab samples and short gravity cores on the adjacent Nile delta shelf (Summerhayes et al., 1978); and dated vibro-core and seafloor data at major, now-submerged archaeological sites of Greek and Roman age seaward of the delta, including major ones in Abu Qir Bay and Alexandria's Eastern Harbor (Bernand and Goddio, 2002; Stanley, 2007; Robinson and Wilson, 2010). Also useful are published analyses of satellite surveys of delta surface and sea-level elevations, deep subsurface stratigraphic and structural data obtained in the northern delta and offshore by means of 2D and 3D geophysical surveys, and associated well core information. These data are compiled by the hydrocarbon (largely gas) companies conducting exploration in this region during the past half-century.

The distance between the delta's southern apex near Cairo and the coast is 160 km, and the delta length along its arcuate coastline is ~270 km, from Alexandria in the west to the margin south of the Gulf of Tineh in the east. Four elongate brackish lagoons, positioned from east to west adjacent to the delta coast (Manzala, Burullus, Idku, and Maryut; Fig. 2A), are of modest depths, ranging to little more than 1 m below msl. They are open to the sea, and their waters are brackish to saline. The delta's coastal margin sequences of Late Pleistocene to present age include Nile fluvial and desert wind-borne sediment, and also those derived from eroded marine sections from nearshore deposits. Sandy delta beaches are in part shaped by the Mediterranean's semi-diurnal microtidal and surge effects, and especially by strong winds that in winter are directed toward the SE. The present coastline's arcuate form results from powerful winter wave surges and wave-driven coastal currents that displace sediment mostly toward the east (Frihy et al., 2002). Coastal material is preferentially eroded from seaward projecting headlands, including the two Nile distributary promontories and the bowed-out coast in the Baltim region (Fig. 2A). This displaced sediment forms the long, narrow sand barriers at the seaward margin of coastal lagoons, while landward-driven masses of wind-blown sand have accumulated as extensive dune fields along the north-central delta coast east of Baltim (Figs. 2A and 2C). A large body of published work summarizes the

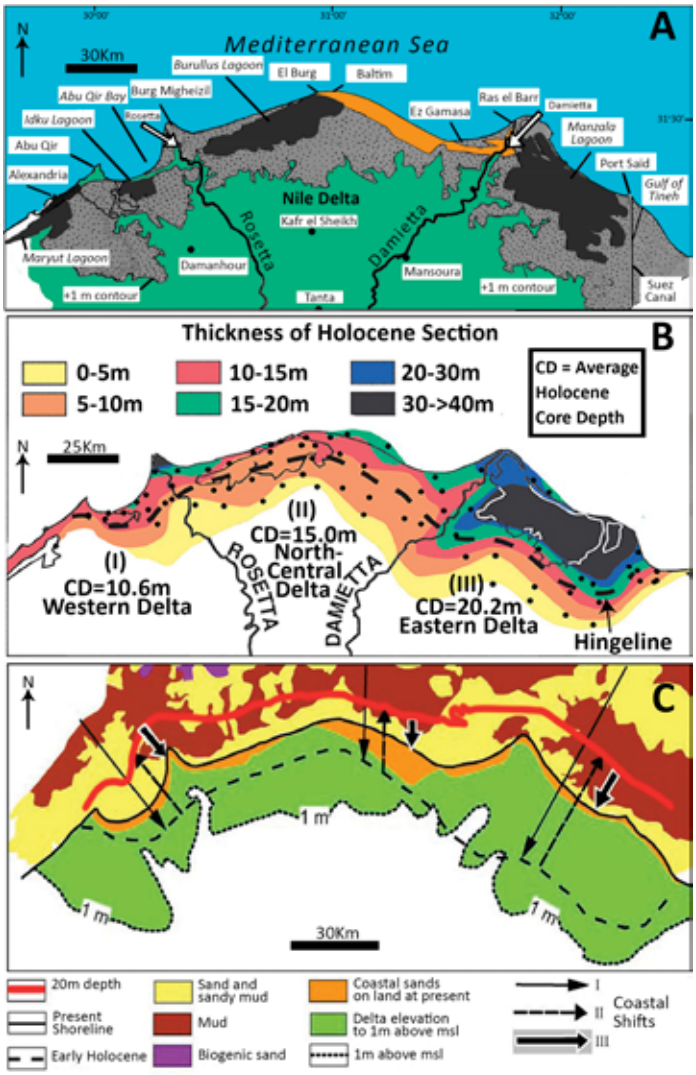

Figure 2. (A) Geographic features and localities in the northern sector of the Nile delta, including those cited in the text. (B) Map showing average thickness (in m) of Holocene section (CD) in sectors I, II, and III of the northern delta. (C) Lithologic aspects and physiographic features in the delta margin and offshore sector. Arrows highlight three major coastal shifts and reversals through time: I, coastline landward retreat in post-glacial time (ca. 16,000 B.C.) to early Holocene (ca. 6000–5500 B.C.); II, coastline seaward advance from early Holocene (ca. 6000–5500 B.C.) to late Holocene (ca. 2500 B.C.); and III, coastline landward retreat, once again, from late Holocene (ca. 2500 B.C.) to present.

results of theoretical modeling and field measurements of sediment displaced from various coastal and offshore shelf sectors and their migration patterns through time (UNDP/UNESCO, 1978; Frihy and El-Sayed, 2013). Teams studying these problems have included several international organizations, the Coastal Research Institute in Alexandria, and other Egyptian research centers and universities. Shoreline stabilization is now partially achieved, at least locally where effective protection measures have been implemented, mostly since the past half-century following closure in 1965 of the Aswan High Dam.

The much-increased role of human activity through time in this region needs to be emphasized. In Predynastic time, from ~5000 B.C. onward, hunters and gatherers in small numbers migrated to the delta from adjoining arid, sand-rich Sahara terrains. The major cultural-ecological shift to irrigation farming and urbanism on the Nile's delta plain, with its available water and organic-rich soil, occurred during the Early Dynastic to Dynastic at ca. 3000 B.C. This evolved to what Butzer (1976) defined as an early hydraulic civilization, a socio-economic system based on deliberate flooding and draining by sluice gates and use of water basins contained by dikes. The major shift in population from the Nile valley northward to the delta took place during the Hellenistic period (323–30 B.C.), a time when Egypt's total population increased to ~5 million (Butzer, 1976).

At present, the country's population has reached ~90 million, with a growth rate above 2.0%/yr. Of this number, ~45–50 million people live in the delta and its proximity and, of these, roughly 20 million are concentrated in and around Cairo at the delta's southern apex, with another 15–20 million occupying the delta's southern and central sectors. About 10 million more people inhabit the northern delta's coastal region; this number includes the 4.5 million people living in Alexandria, Egypt's second largest city and its major port and industrial center. Population densities are extremely high (to 1000 or more/km^2) in much of the Nile delta and valley, two sectors that comprise areas of 22,000 km^2 and 13,000 km^2, respectively, and that together form only ~3.5% of Egypt's total area. Due to anthropogenic stresses, the Nile delta has been modified to the extent that it no longer functions as a natural fluvial-marine depocenter (Stanley and Warne, 1998).

NEOTECTONIC EFFECTS

Neotectonics refers broadly to active seismicity and tectonic movements that are geologically recent, from the Tertiary onward and continuing to the present. Considerable information on seismicity and tectonics affecting the delta's surface and subsurface sequences has been published in recent years, following active exploration at the delta's hydrocarbon provinces. Data has been obtained from 2D and 3D seismic surveys, along with well core analysis, in the northern delta and offshore shelf. These and seismograph monitoring stations have helped clarify the relation between Holocene sediment deposits and their displacement by earthquakes, faults, and delta surface lineaments, the latter mapped by Landsat. Although identified as a passive margin, northern Egypt is characterized by frequent earthquake events of shallow origin and small magnitude (M of 3 or less) and of moderate quakes (M to 5) that occur less frequently (Korrat et al., 2005). Earthquake and fault patterns are interpreted as results of ongoing interactions among African, Arabian, and Eurasian plates and the Sinai subplate.

Two active linear belts cross Egypt and intersect in the delta: a SE to NW Gulf of Suez-Cairo-Alexandria trend and a NE to SW Eastern Mediterranean-Cairo-Fayum trend (Fig. 3A), with slip faults associated with these megashears (Kebeasy, 1990; Gamal, 2013). Earthquakes related to major trends include those that recently affected the Cairo area (in 1992, M = 5.9), and the Alexandria to offshore sector (in 1998, M = 6.7); the latter initiated at a depth of 28 km. Alexandria, in particular, is a high earthquake risk zone that has periodically experienced considerable damage, such as the powerful quake and associated tsunami recorded in 365 A.D. that destroyed much of the city (Guidoboni et al., 1994), and major quakes in 1303 and 1323 A.D. that damaged the famous Alexandria lighthouse. There is evidence of seismic damage and fault offset in Alexandria that have disturbed ancient construction and also recently tilted some buildings. Modern earthquakes with M ≥5 occur about every 23 years. Although most quakes are of lower seismicity, together they constitute a source of seismic hazard for the many who live in the delta and its coastal margin (El-Ela et al., 2012).

An E-W–trending series of faults crosses the northern delta and form a hingeline or hinge zone (Fig. 3B) that separates a southern delta block from a northern delta block. It is defined by step faults and gravity-induced displacements associated with down-to-north rotated fault blocks that extend from deep structural offsets to the surface. Geophysical surveys show that such features mapped in subsurface on land in the northern delta block continue at depth offshore (Sharaf et al., 2014). Ground motion measurements indicate that these can affect both surface deposits of the northern delta and seafloor strata offshore (Mohamed et al., 2015).

Tectonic activity associated with reactivation of faults at depth can cause structural displacements that in some cases extend upward to Late Pleistocene and Holocene surface deposits (Fig. 3C). Surveys have shown a close relation between underlying structural patterns and some delta plain surface lineaments, faults, and earthquakes (Elmahdy and Mohamed, 2016). By offset and subsidence, in part from isostatic loading and readjustments of strata at depth, the northern delta–offshore shelf sector has accumulated up to 3500 m of underlying stratigraphic section since the late Miocene (Fig. 3C); the depth to basement rock is 9–10 km (Kellner et al., 2009). Tectonic effects in this region at times have exceeded those of eustatic factors in controlling coastline evolution (Sarhan, 2015), such as at the NE delta coast in the Manzala lagoon area. This may be caused by pull-apart basin development (Stanley, 1990) where a much thicker Holocene sequence (to ~50 m) of mud-rich deposits accumulated beneath the present shallow, elongate lagoon (Fig. 2B).

Petrologic examination of well core sections records examples of post-depositional faulting, slumping, and sediment deformation (Rizzini et al., 1978). Features such as convolute bedding of mud- and silt-rich deposits suggest processes associated with sediment dewatering and liquefaction. Likely triggers are earthquake tremors that can generate high excess pore-water pressure within unconsolidated subsurface and surface deposits. Examples of recent earthquake-triggered liquefaction were recorded at ground surface shortly following the 1992

Cairo earthquake where water-saturated silty to sandy soil had been shaken and failed near the epicenter (El-Gamal et al., 1993). Similar features at shallow depths in the delta's Holocene unconsolidated deposits near the coast (Fig. 4B), some of which probably also failed by recent neotectonic motion and liquefaction, are illustrated in the following section.

COMPACTION AND SUBSIDENCE

Sediment compaction rates are calculated for the Holocene sections in 85 drill cores landward of the coast. Radiocarbon dates in most cores provide a temporal framework for interpreting these sediment sections. Compaction rates were determined by measuring the thicknesses of individual strata in each meter of drilled Holocene deposits between the delta surface and basal section at each core site so as to measure average thicknesses per meter and for the entire core at each site. A total of 3183 layers in cores were thus examined to determine if any systematic down-core temporal and spatial-regional thickness patterns in the northern delta could be detected (Stanley and Corwin, 2013). Thickest layers are almost always recorded in the top 1–2 m of section and dated to <1000 yr in age; the next few meters below this upper section record considerably thinner strata. This observation is attributed to expulsion of interstitial pore water by compression from sediment overburden and by evaporation in near-surface deposits in this arid setting (100–250 mm rainfall/yr). Strata thicknesses tend to decrease irregularly to depths of 5–6 m during the upper to mid-Holocene, and from those depths downward they continue to thin more gradually from mid- to basal Holocene sections. Strata thickness reduction rates, calculated by derivatives of regression curves, are treated as proxy for compaction rate (Stanley and Corwin, 2013). By mid-core depths, >50% of total Holocene core compaction is accounted for by strata thickness reduction. These patterns of down-core stratal thinning are observed all along the northern delta plain and prevail independently of original depositional environment and total thickness of Holocene section.

This strata thickness method shows that average rates of compaction (ARC) measured for total Holocene sections vary regionally along the delta margin, increasing as follows (Fig. 4A): ~3.7 mm/yr in NW sector (I); ~7.7 mm/yr in the NC sector (II); and ~8.4 mm/yr in the NE sector (III). Measurement of upper strata compaction per meter provides results that parallel those of land subsidence measurements made by recent satellite surveys (El-Asmar et al., 2012). For example, high subsidence rates, to ~8 mm/yr, were measured for sectors between Baltim and Manzala lagoon (Becker and Sultan, 2009). Satellite imagery techniques (radar interferometry) identified coastal sectors of accelerated subsidence in areas of Holocene sections subject to high depositional rates, including the Rosetta, Baltim, and Damietta headlands (Fig. 2A). To determine rates of relative sea level, ARC measurements are added to those of eustatic sea-level rise; these latter presently range from 2.6 to 3.3 mm/yr since ~2000 A.D. (cf. Shaltout et al., 2015; Hansen et al., 2016). Of note, an average eustatic rise of 3 mm/yr would account for only ~26% to 45% of total relative sea-level rise rates between NE delta sector III and NW delta sector I.

Measurement of sand, silt, and clay proportions in Holocene core samples (Stanley and Clemente, 2014) indicate that relative

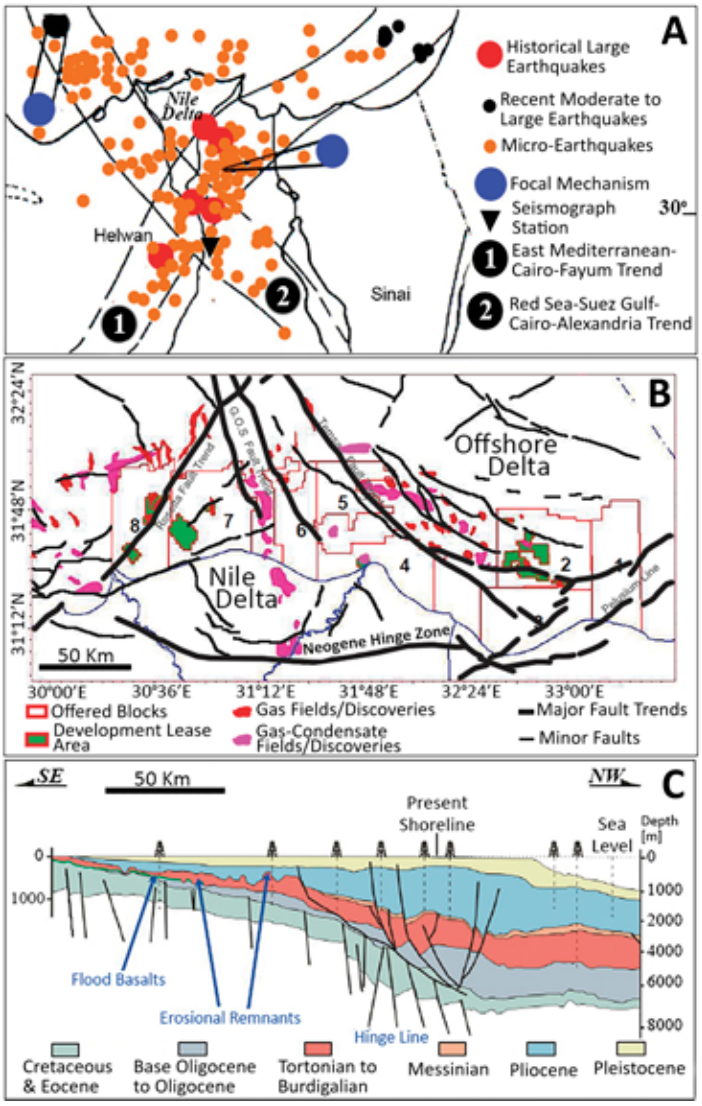

Figure 3. (A) Recent earthquake epicenters in the Nile delta and northern Egypt, emphasizing two active megashears discussed in text: (1) East Mediterranean-Cairo-Fayum Trend, and (2) Red Sea-Gulf of Suez-Alexandria Trend (modified after Kebeasy, 1990, and Gamal, 2013). (B) The depocenter's coastal margin showing gas field discoveries and major structural trends both on- and offshore, including the pronounced Neogene Hinge Zone trending E-W across the northern delta (after EGAS, 2015). G.O.S.—Gulf of Suez. (C) SE to NW cross section highlighting subsurface stratigraphy and major subsurface structural trends from delta to offshore shelf, including some that extend to the delta surface (after Kellner et al., 2009).

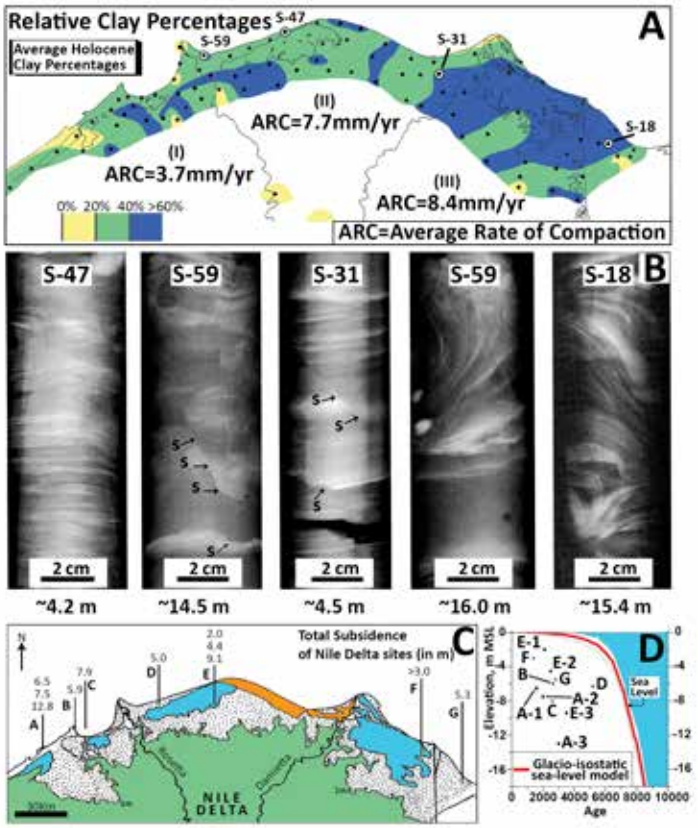

Figure 4. (A) Map showing distribution of average relative percentages of clay in Holocene sections and average rates of compaction (ARC) in mm/yr across three northern delta sectors (I, II, III); dots indicate sites of 85 sampled drill cores (after Stanley and Clemente, 2014). (B) X-radiographs of selected drill cores sections (locations shown in A): horizontal laminations in S-47; fault-like shears(s) in S-31 and S-59; and convoluted strata units in S-18 and S-59. Scale = 2 cm. (C) Location of seven submerged sites with archaeological material; the 11 numbers indicate depths (in m) of materials below present sea level (after Stanley and Toscano, 2009). (D) Plotted age and depth of submerged materials in C show all lie well below the Eastern Mediterranean sea-level curve of Sivan et al. (2001), recording continued margin subsidence.

percentages of clay are highest (40%–60%) in the N and NE sectors (II, III) where high ARC values range from 7.7 to 8.4 mm/yr (Fig. 4A). This finer-grained sediment fraction is preferentially displaced by currents toward the NE delta margin (arrows in Fig. 5A). It is likely that water-saturated, clay-rich sediments readily expulsed much of their interstitial pore water shortly after burial by successive deposits and evaporation. In X-radiographs of Holocene delta core sections, most displaying well-defined horizontal bedding (Fig. 4B, section S-47), there are examples of interbedded strata that have been extensively disturbed. Some display convolute stratification (Fig. 4B, in sections S-18 and S-59), interpreted as having failed by liquefaction and upward expulsion of interstitial water. Other disturbed strata record sharp, fault-like shear offsets (Fig. 4B, arrows and symbol S in S-31 and S-59). Because such layers generally occur between horizontal strata above and below them, they likely record the effects of natural episodic disturbance events. Some may have formed by rapidly increased sediment accumulation and overloading. Others perhaps resulted from recent earthquake tremors and ground motion, or from tectonic shifts and reorganization of underlying strata at depth, as cited in the previous section. Similarly, human-triggered effects also occur in areas where delta surfaces have been artificially lowered to ~1 m or more and that are affected locally by liquefaction as a result of hydrocarbon and groundwater extraction.

DECREASED SEDIMENT REPLENISHMENT

An ample sediment supply provided regularly to a delta's margin helps minimize or moderate problems of coastal submergence by eustatic sea-level rise and land subsidence triggered by neotectonics and/or sediment compaction as discussed above. This balance no longer occurs sufficiently at the Nile delta's coastal sector where amounts of discharged water and sediment have diminished markedly in recent time due to altered climatic conditions and much increased human impacts. Without addition of much needed superposed deposits at the coast, the youngest (earlier than 1000 A.D.), uppermost water-saturated sediment layers are now being lowered at a more rapid rate relative to sea level (Figs. 4C and 4D).

The Nile's present total flow is contributed by relatively small, isolated areas in the East African lake region and the Ethiopian highlands. The high precipitation at the headland of the White Nile is distributed between two rainfall seasons. Water of the White Nile enters the Sudd marshes and seasonally flooded areas to the north, where evaporation greatly exceeds rainfall; this results in an outflow from the wetlands that is only about half that of inflow (Sutcliffe and Parks, 1999). In marked contrast, the Ethiopian mountains, with their high rainfall in a single season and steep topography, produce larger runoffs and more concentrated flows in the Blue Nile and Atbara during shorter periods.

During much of the Holocene, amounts of sediment transported from upland Nile sources and dispersed northward to the delta margin have been largely controlled by Nile hydrologic attributes responding to major long-term climatic variations. Strong rains prevailed, especially during the latest Pleistocene-Holocene Wet Phase that, in Ethiopia, lasted ~6500 yr, between ca. 9000 B.C. and ca. 2500 B.C. (Said, 1993, his figure 2.12). The rain-front at that time shifted northward 8–10 degrees in the Nile Basin, over arid sectors of the Sahel and sectors of the Sahara in the Sudan and Egypt. Such rainfall patterns responded largely to fluctuation of the Inter-Tropical Convergence Zone (ITCZ) that induced major Nilotic hydrologic and sedimentation changes due to low-latitude isolation forcing over long periods. On a shorter (sub-millennial) scale, Nile valley climatic input by El Niño Southern Oscillations (ENSO) were also influential (Said, 1993; Marriner et al., 2012). During the African humid phase, strong boreal summer insulation produced higher rainfall in northern

Africa, which led to important tributary (wadi) input into the lower Main Nile valley that accounted for 40%–50% of total fluvial water and much-increased sediment loads.

The Wet Phase, ending at ca. 2500 B.C., was followed to the present by an Arid Phase (Said, 1993). Nile tributary input ceased, while the Main Nile received a larger proportion of Blue Nile and Atbara contributions. Ethiopian highlands presently supply by far the largest proportions of Nile water (Blue Nile: 59%; Atbara River: 13%; Sobat: 14%) and sediment transported northward across the Sudan and Egypt. The White Nile, flowing across parts of eight countries (Fig. 1), provides only 28% of the total Nile water supply, of which about half of this amount (14%) is contributed by the Sobat, one of its tributaries with a source in Ethiopia. The Blue and White Niles and Atbara join to form the Main Nile in the Sudan (Woodward et al., 2015), and this fluvial system then continues in its channel that crosses desert terrains of both the Sudan and Egypt to the delta. North of the delta's apex near Cairo, most Nile waters are now diverted into a complex irrigation system comprising hundreds of kilometers of canals and drains (Fig. 5A).

Anthropogenic pressures have increased continuously, especially during the past two centuries, and now dominate the hydrographic system. Barrages (Assyut, Naga Hamadi, Esna) emplaced on the Nile during the nineteenth century, the first dam at Aswan (Low Dam) in 1902, and water diversion systems along the Nile valley had already modified water delivery to lower Egypt by the turn of the twentieth century. Two mid-1900s dams in the northern delta, one constructed at Edfina on the Nile's Rosetta branch and the other at Faraksour Sudd on the Damietta branch, prevent water in these two now much-altered distributaries from reaching the coast (Fig. 2A). The High Aswan Dam was then constructed in 1965 to release Nile water throughout the year instead of during the short flood season in summer. It is backed by the enormous Lake Nasser reservoir (area of 5250 km^2; length of 510 km), with a large water loss (12%–14% of annual input) from evaporation and seepage. Consequently, the total amount of water flowing below the High Dam and to the delta is considerably reduced. About 84 Bm^3 of useable fresh water remain, of which

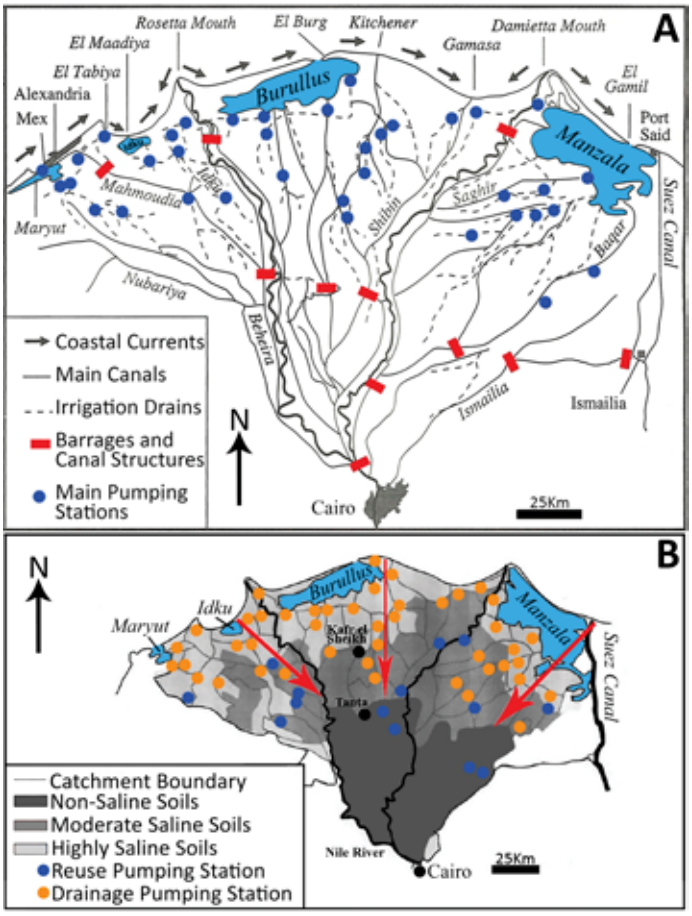

Figure 5. (A) Map of geographic features and network of major canals, drains, and pumping stations in the Nile delta (modified after Sestini, 1992); arrows at coast show dominant east-directed wave-driven current flow (after various authors). (B) Map of delta soil salinities (non-saline = <1000 ppm; moderate-mixed saline = 1000–35,000 ppm; highly saline = 35,000 ppm), highlighting the southward progressing saline intrusion (modified after Sefelnasr and Sherif, 2014).

55.5 Bm^3 is reserved for Egypt. At present, a large fraction of Nile sediment that once accounted for ~100 million tons deposited below Aswan is now trapped in the southern part of the reservoir, where it has been forming a new lacustrian delta since the High Dam closure.

Several other large-scale projects under construction include those to divert large volumes of Nile water to convert arid, saline areas into agricultural land: one to bring water from Lake Nasser to oases in Egypt's Western Desert (Toshka–New Valley Project); another is to distribute water across the northern Sinai (Al-Salam Canal Project). Moreover, dams and barrages have been built in the Sudan and Ethiopia. Most of the now-limited volume of Nile water that reaches the delta is diverted and channelized into the complex water distribution system, most utilized for agricultural, municipal, and industrial needs. Egypt now releases less than 10% of its water supply, a mostly saline and highly polluted aqueous mix, to the sea, with little sediment available for coastal replenishment. Egypt, the tenth and last country below Nile headwaters, presently needs much more fresh water than can be provided by the Main Nile. Without it, the delta's coastal margin, for the most part depleted of its former sediment supply for replenishment, continues to erode locally and subside.

PROGNOSTICS

A minimal relative sea-level rise of ~100 cm is predicted between now and the year 2100 at the Nile delta's coast, where laterally variable but continued ~6.7 to ~11.4 mm/yr rates of submergence have been measured. This takes into account average rates of sediment compaction leading to subsidence of ~3.7 to 8.4 mm/yr (NW to NE delta rates) added to the

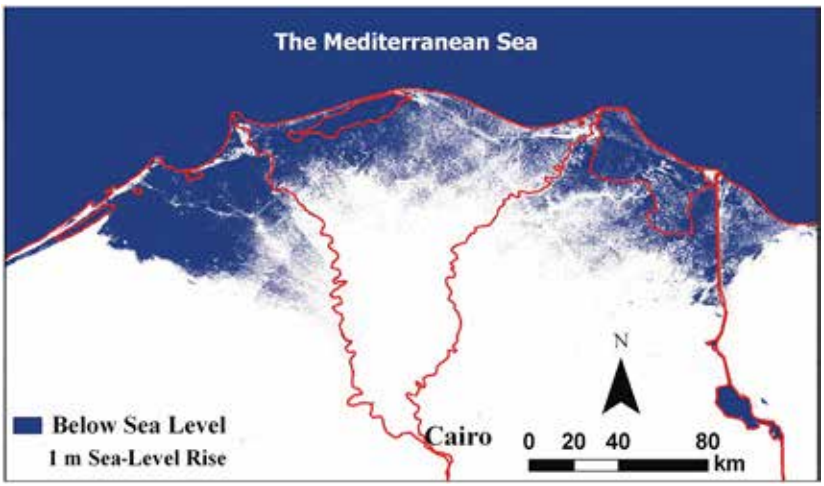

Figure 6. The present rate of relative sea-level rise as calculated in this analysis will reach ~1 m above mean sea level (msl) by 2100 A.D., with marine water (shown in blue) having advanced landward, submerging about one-third of the present Nile delta surface (after Hereher, 2010).

eustatic sea-level rise of ~3 mm/yr. A total relative sea-level rise of 1 m or more could well occur at this delta's low margin, but not by eustatic rise alone, which accounts for only ~26% to 45% of measured total estimated relative sea-level rise (~6.7 mm/yr to ~11.4 mm/yr) between the delta's NW and NE coastal margin. Total relative sea-level rise by year 2100 could be further increased locally by neotectonic lowering as has occurred sporadically and affected the delta's margin in the recent past. Additional repercussions are envisioned from the effects of a continued decrease of Nile sediment now reaching the coast, resulting from increased anthropogenic entrapment by new up-river dams and other structures, plus increased rates of eustatic rise in sea level due to higher rates of polar ice melt that, in years ahead, may possibly accompany global warming.

Land subsidence plus eustatic sea-level rise presently affect saline water intrusion into the delta's aquifer. Highly saline soils in the northern delta become moderately saline southward from about Kafer el-Sheikh to the central delta (Fig. 5B). Non-saline soils occur primarily south of Tanta, in the central to southern delta (Kotb et al., 2000; Sefelnasr and Sherif, 2014). Egypt could help ameliorate these salinization and coastal erosion problems by constructing laterally extensive, continuous, and deeply emplaced protection structures along the delta's coastal perimeter. Present ongoing quarrying of sand dunes along the delta coast, for mineral mining and other applications, should be avoided, because it removes a natural protective barrier that backs the low-lying shoreline. Governmental investment in establishing much-needed desalination plants and drip irrigation technology should be planned. Serious indeed is decreasing agricultural production at a time when Egypt's population continues to increase. Further Nile fresh water decrease would be grave because, at best, the river barely supplies 97% of Egypt's water needs, and now provides only 660 m^3, one of the world's lowest per capita water shares. With a population expected to double in the next 50 years, Egypt is projected to reach a state of serious country-wide fresh water and energy shortage by 2025.

Additional complications include international accords with regard to the Nile's hydrology, drawn up in 1929 and amended in 1959, that attributed most Nile water to Egypt and Sudan without consulting upstream states (Waterbury, 1979; Said, 1993). To address its own conditions of drought and energy poverty, Ethiopia began construction of its Grand Ethiopian Renaissance Dam (GERD) in 2011, with completion expected this year. The dam, paid for mainly by Ethiopia, but with aid from other countries, will be Africa's largest hydroelectric power plant, producing 6000 megawatts of electricity with 16 turbines and an estimated production of 15,000 GwH per year. The reservoir behind the dam will flood 1680 km^2, retain a volume of ~63 Bm^3, and could take 5–7 years to reach capacity. During this period of fill, the Nile's fresh water flow to Egypt may be cut by 25%, with a loss of a third of the electricity generated by the Aswan High Dam.

In addition to the GERD, Ethiopia is proposing more dams along the Nile, and a new series of dams is also planned in the Sudan. With ~400 million people living in the 10 countries across which the Nile flows (Fig. 1), some now experiencing severe droughts and unmet energy needs, it is expected that a large proportion of Nile water now directed to Egypt (~70%; Said, 1993), will have to be reallocated up-river (Fig. 6). Already facing a multitude of economic, political, and demographic problems (Fragile States Index, 2016), in addition to hydrological and coastal protection challenges, the interdependence of the Nile Basin countries and their reliance upon the Nile's waters must be resolved immediately. It is hoped that rather than resorting to threats and military action, some form of arbitration by regional or global bodies be applied to the delicate situation, especially with regard to the three most impacted countries along the Blue Nile: Egypt, the Sudan, and Ethiopia.

ACKNOWLEDGMENTS

Prof. M.P. Bernasconi, University of Calabria, Prof. P. Eager, Hood College, K. Corwin, Idaho State University, A.N. Ellis, Adamstown, Maryland, and two anonymous reviewers are sincerely thanked for their valuable assistance with this article. Messrs. L. Vianello and G. Contardi, staff of Salini Impregilo, S.p.A., kindly shared photographs and information about the GERD dam's construction in Ethiopia. Research funding to the senior author and the Mediterranean Basin (MEDIBA) Program that led to this synthesis was provided by the Smithsonian Institution, National Museum of Natural History, Washington, D.C.

REFERENCES CITED

Attia, M.I., 1954, Deposits in the Nile Valley and the Delta: Cairo, Geological Survey of Egypt, 356 p.

Becker, R.H., and Sultan, M., 2009, Land subsidence in the Nile Delta: Inferences from radar interferometry: The Holocene, v. 19, no. 6, p. 949–954, doi: 10.1177/0959683609336558.

Bernand, A., and Goddio, F., 2002, L'Égypte Engloutie—Alexandrie: London, Arcperiplus Publishing, 191 p.

Butzer, K.W., 1976, Early Hydraulic Civilization in Egypt: A Study in Cultural Ecology: Chicago, Illinois, The University of Chicago Press, 134 p.

EGAS, 2015, EGAS Concessions Map and 2015 International bid round blocks: Ministry of Petroleum and Mineral Resources Technical Report (1) 8, Exploration Blocks, p. 1–5.

El-Asmar, H.M., Hereher, M.E., and El-Kafrawy, S.B., 2012, Threats facing lagoons along the north coast of the Nile Delta, Egypt: International Journal of Remote Sensing Applications, v. 2, no. 2, p. 24–29.

El-Ela, A.A.M., El-Hadidy, M., Deif, A., and Elenean, A., 2012, Seismic hazard studies in Egypt: NRIAG Journal of Astronomy and Geophysics, v. 1, no. 2, p. 119–140, doi: 10.1016/j.nrjag.2012.12.008.

El-Gamal, A.W., Adalier, K., and Amer, M., 1993, Liquefaction during the October 12, 1992, Egyptian Dahshure earthquake: Proceedings: Third International Conference on Case Histories in Geotechnical Engineering, St. Louis, Missouri, June 1–4, 1993, paper no. 14.18.

Elmahdy, S.I., and Mohamed, M.M., 2016, Mapping of tecto-lineaments and investigate their association with earthquakes in Egypt: A hybrid approach using remote sensing data: Geomatics, Natural Hazards & Risk, v. 7, no. 2, p. 600–619, doi: 10.1080/19475705.2014.996612.

Fragile States Index, 2016, Fund for Peace, 1101 14th Street NW, Suite 1020, Washington, D.C. 20005, http://library.fundforpeace.org/fsi16-report (last accessed 5 Dec. 2016).

Frihy, O.E., and El-Sayed, M.Kh., 2013, Vulnerability risk assessment and adaptation to climate change induced sea level rise along the Mediterranean coast of Egypt: Mitigation and Adaptation Strategies for Global Change, v. 18, no. 8, p. 1215–1237, doi: 10.1007/s11027-012-9418-y.

Frihy, O.E., Debes, E.A., and El Sayed, W.R., 2002, Processes reshaping the Nile delta promontories of Egypt: Pre- and post-protection: Geomorphology, v. 1284, p. 1–17, doi: 10.1016/S0169-555X(02)00318-5.

Gamal, M.A., 2013, Truthfulness of the existence of the Pelusium Megashear fault system, East of Cairo, Egypt: International Journal of Geosciences, v. 4, p. 212–227, 10.4236/ijg.2013.41018.

Guidoboni, E., Comastri, A., and Traina, G., 1994, Catalogue of Ancient Earthquakes in the Mediterranean Area up to the 10th Century: Rome, Bologna, Istituto Nazionale di Geofisica, 504 p.

Hansen, J., Sato, M., Hearty, P., Ruedy, R., Kelley, M., Masson-Delmotte, V., Russell, G., Tselioudis, G., Cao, J., Rignot, E., Velicogna, I., Tormey, B., Donovan, B., Kandiano, E., von Schuckmann, K., Kharecha, P., Legrande, A.N., Bauer, M., and Lo, K.-W., 2016, Ice melt, sea level rise and superstorms: Evidence from paleoclimate data, climate modeling, and modern observations that 2 °C global warming could be dangerous: Atmospheric Chemistry and Physics, v. 16, p. 3761–3812, doi: 10.5194/acp-16-3761-2016.

Hereher, M.E., 2010, Vulnerability of the Nile Delta to sea-level rise: An assessment using remote sensing: Geomatics, Natural Hazards and Risk, v. 1, no. 4, p. 315–321, doi: 10.1080/19475705.2010.516912.

Kebeasy, R.M., 1990, Seismicity, *in* Said, R., ed., The Geology of Egypt: Rotterdam, A.A. Balkama, p. 51–59.

Kellner, A., Brink, G.J., El-Khawaga, H., Brink-Larsen, S., Maksoud, H., El Saad, A., Atef, A., Young, H., and Finlayson, B., 2009, Depositional history of the West Nile Delta—Upper Oligocene to Upper Pliocene: Adapted from oral presentation at AAPG International Conference and Exhibition, Cape Town, South Africa, 26–29 October 2008.

Korrat, I.M., El Agami, N.L., Hussein, H.M., and El-Gabry, M.N., 2005, Seismotectonics of the passive continental margin of Egypt: Journal of African Earth Sciences, v. 41, p. 145–150, doi: 10.1016/j.jafrearsci.2005.02.003.

Kotb, T.H.S., Watanabe, T., Ogino, Y., and Tanji, K., 2000, Soil salinization in the Nile delta and related policy issues in Egypt: Agricultural Water Management, v. 43, no. 2, p. 239–261, doi: 10.1016/S0378-3774(99)00052-9.

La Guardia, A., 2016, Special Report: The Arab world: The clash within a civilization: The Economist, v. 419, no. 8989, p. 1–16, http://www.economist.com/news/special-report/21698444-hundred-years-after-sykes-picot-agreement-carved-up-ottoman-empire-new-arab (last accessed 28 Nov. 2016).

Marriner, N., Flaux, C., Kaniewski, D., Morhange, C., Leduc, G., Moron, V., Chen, Z., Gasse, F., Empereur, J.-Y., and Stanley, J.-D., 2012, ITCZ and ENSO-like pacing of Nile delta hydro-geomorphology during the Holocene: Quaternary Science Reviews, v. 45, no. 8, p. 73–84, doi: 10.1016/j.quascirev.2012.04.022.

Mohamed, A.A., Helal, A.M.A., Mohamed, A.M.E., Shokry, M.M.F., and Ezzelarab, M., 2015, Effects of surface geology on the ground-motion at New Borg El-Arab City, Alexandria, northern Egypt: NRIAG Journal of Astronomy and Geophysics, v. 5, no. 1, p. 55–64, doi: 10.1016/j.nrjag.2015.11.005.

Rizzini, A., Vezzani, F., Cococcetta, V., and Milad, G., 1978, Stratigraphy and sedimentation of a Neogene Quaternary section in the Nile Delta area (A.R.E.): Marine Geology, v. 27, no. 3–4, p. 327–248.

Robinson, D., and Wilson, A., eds., 2010, Alexandria and the North-Western Delta: Oxford, Oxford Centre for Maritime Archaeology, Monograph 5, 282 p.

Said, R., 1993, The River Nile: Geology, Hydrology, and Utilization: Tarrytown, New York, Pergamon Press, 320 p.

Sarhan, M.A., 2015, High resolution sequence stratigraphic analysis of the Late Miocene Abu Madi Formation, northern Nile Delta basin: NRIAG Journal of Astronomy and Geophysics, v. 4, p. 298–306, doi: 10.1016/j.nrjag.2015.11.003.

Sefelnasr, A., and Sherif, M., 2014, Impacts of seawater rise on seawater intrusion in the Nile Delta aquifer, Egypt: Ground Water, v. 52, no. 2, p. 264–276, doi: 10.1111/gwat.12058.

Sestini, G., 1992, Implications of climatic changes for the Nile delta, *in* Jeftic, L., Millimam, J.D., and Sestini, G., eds., Climate Change and the Mediterranean: London, Edward Arnold, p. 535–557.

Shaltout, M., Tonbol, K., and Omstedt, A., 2015, Sea-level change and projected future flooding along the Egyptian Mediterranean coast: Oceanologia, v. 57, p. 293–307, doi: 10.1016/j.oceano.2015.06.004.

Sharaf, E., Korrat, I., Seisa, H., and Esmaiel, E., 2014, Seismic imaging and reservoir architecture of sub-marine channel systems offshore west Nile Delta of Egypt: Open Journal of Geology, v. 4, p. 718–735, doi: 10.4236/ojg.2014.412052.

Sivan, D., Wdowinski, S., Lambeck, K., Galili, E., and Raban, A., 2001, Holocene sea-level changes along the Mediterranean coast of Israel, based on archaeological observations and numerical model: Palaeogeography, Palaeoclimatology, Palaeoecology, v. 167, no. 1–2, p. 101–117, doi: 10.1016/S0031-0182(00)00234-0.

Stanley, J.-D., 1990, Recent subsidence and northeast tilting of the Nile delta, Egypt: Marine Geology, v. 94, no. 1–2, p. 147–154, doi: 10.1016/0025-3227(90)90108-V.

Stanley, J.-D., ed., 2007, Underwater Archaeology in the Canopic Region in Egypt. Geoarchaeology: Oxford, Oxford Centre for Maritime Archaeology, Monograph 2, Institute of Archaeology, 128 p.

Stanley, J.-D., and Clemente, P.L., 2014, Clay distributions, grain sizes, sediment thicknesses, and compaction rates to interpret subsidence in Egypt's northern Nile Delta: Journal of Coastal Research, v. 30, no. 1, p. 88–101, doi: 10.2112/JCOASTRES-D-13-00146.1.

Stanley, J.-D., and Corwin, K.A., 2013, Measuring strata thicknesses in cores to assess recent sediment compaction and subsidence of Egypt's Nile delta coastal margin: Journal of Coastal Research, v. 29, no. 3, p. 657–670, doi: 10.2112/JCOASTRES-D-12A-00011.1.

Stanley, J.-D., and Toscano, M.A., 2009, Ancient archaeological sites buried and submerged along Egypt's Nile delta coast: Gauges of Holocene delta margin subsidence: Journal of Coastal Research, v. 25, no. 1, p. 158–170, doi: 10.2112/08-0013.1.

Stanley, J.-D., and Warne, A.G., 1998, Nile Delta in its destruction phase: Journal of Coastal Research, v. 14, no. 3, p. 794–825.

Stanley, J.-D., McRea, J., and Waldron, J., 1996, Nile Delta Drill Core and Sample Database for 1985–1994: Mediterranean Basin (MEDIBA) Program: Smithsonian Contributions to the Marine Sciences, doi: 10.5479/si.01960768.37.1.

Summerhayes, C.P., Sestini, G., Misdorp, R., and Marks, N., 1978, Nile Delta: Nature and evolution of continental shelf sediments: Marine Geology, v. 27, no. 1–2, p. 43–65, doi: 10.1016/0025-3227(78)90073-7.

Sutcliffe, J.V., and Parks, Y.P., 1999, The Hydrology of the Nile: Oxford, UK, International Association of Hydrological Sciences, 179 p.

UNDP/UNESCO, 1978, Arab Republic of Egypt: Coastal Protection Studies, Project Findings and Recommendations. UNDP/EGY/73/063 Final Report, Paris, FNR/SC/OSP/78/230, 483 p.

Waterbury, J., 1979. Hydropolitics of the Nile Valley: Syracuse, New York, Syracuse University Press, 301 p.

Woodward, J., Macklin, M., Fielding, L., Millar, I., Spencer, N., Welsby, D., and Williams, M., 2015, Shifting sediment sources in the world's longest river: A strontium isotope record for the Holocene Nile: Quaternary Science Reviews, v. 130, p. 124–140, doi: 10.1016/j.quascirev.2015.10.040.

Manuscript received 13 July 2016
Revised manuscript received 29 Oct. 2016
Manuscript accepted 17 Nov. 2016